npj | heritage science

Article

https://doi.org/10.1038/s40494-025-01604-2

Determining the condition of waterlogged archaeological woods and iron nails from the Yenikapı 17 shipwreck using multiple analytical techniques

Check for updates

Namık KILIÇ

Nineteen waterlogged wood (WAW) samples from the YK 17 shipwreck, focusing on pine and oak species, were initially investigated using basic techniques, including maximum water content (MWC), basic density (BD), and relative basic density (RBD), to provide comprehensive insights into their degradation state. The wood samples were classified as Class I, with oak WAW samples exhibiting higher MWC values compared to those of pine. Additionally, minimally invasive methods, including Fourier Transform Infrared Spectroscopy (FTIR), scanning electron microscopy (SEM), and SEM-energy-dispersive X-ray spectroscopy (EDS), were utilized for the physical and chemical characterization of the WAW samples. FTIR analysis revealed significant chemical degradation, evidenced by the absence of cellulose and hemicellulose peaks, while lignin components demonstrated greater durability. SEM imaging illustrated the physical deterioration of the wood cells, confirming the destruction of the S2 layer and the disintegration of tracheids. Furthermore, elemental analysis via SEM-EDS identified contamination by calcium, iron, and sulphur, likely attributable to the marine environment and associated iron nails. Finally, X-ray diffraction (XRD) analysis of the four iron nails provided the first assessment of their chemical composition, revealing the presence of goethite and calcite in highly corroded samples. Among these findings, the conservation process of the Yenikapı (YK) 17 shipwreck can be performed more successfully, and the study serves as a notable case study that highlights the complexities and approaches involved in the conservation of WAW.

The conservation of archaeological wooden artifacts, particularly those submerged in water, poses significant challenges due to the natural degradation processes associated with waterlogged environments. Wooden shipwrecks have a significant place in this cultural heritage group. The wood of the shipwrecks becomes waterlogged during burial underwater or wetlands. Waterlogged archaeological wood (WAW) tends to degrade as it becomes saturated with water, leading to the breakdown of its cellular structure and the loss of mechanical properties. The interaction of microorganisms, fungal decay, and chemical reactions with saline and fresh water can further exacerbate this degradation, resulting in extensive damage that compromises the structural integrity of wooden remains[1–4].

Consequently, understanding the degradation mechanisms of waterlogged wood is crucial in conservation efforts and for interpreting the maritime archaeological findings. The degradation condition of WAW is influenced by several factors, such as wood species, its state before burial and burial conditions[5,6]. Although each analysis may have its limitations when used individually, the development of multi-disciplinary diagnostic analyses over the past few decades has enabled a more accurate assessment of the degradation condition of WAW. The evaluation of the physical degradation of the WAW allows for the determination of the effects of decay caused by mass loss. This situation results in an increase in the porosity of the wood and a rise in its water content[7,8]. Typically, the standard methods for measuring the physical parameters of WAW include maximum water content (MWC) and basic density (BD)[9–11]. In addition to these techniques, relative basic density (RBD) can be calculated to evaluate the impact of wood species on the degradation mechanism of WAW[12].

The primary components of wood are polymeric substances: cellulose, hemicellulose, and lignin. The composition and proportions of these

Department of Conservation of Marine Archaeological Objects, İstanbul University, İstanbul, Türkiye. e-mail: namik.kilic@istanbul.edu.tr

polymers vary based on the wood species, the type of wood cell, and the specific areas within the cell wall[13]. Among various methodologies, The Fourier transform infrared spectroscopy (FTIR) analysis stands out as particularly promising due to its quick execution, low sample requirements, and the substantial expertise gained from its application. The analysis performed to examine the chemical structure of the WAW enables the quantitative assessment of the residual components present in wood cells, thereby facilitating a comprehensive understanding of the ultimate effects of degradation on the material. This analytical approach is essential for evaluating how degradation alters the structural integrity and properties of wood over time. Another notable benefit of this technique is its effectiveness in conducting analyses with tiny samples using ATR attachment. Another noteworthy benefit of this technique is its effectiveness in conducting analyses with small samples[14–18].

Microscopy techniques, including light and electron microscopy, play a crucial role in characterizing the extent and location of degradation at both cellular and subcellular levels. Notably, scanning electron microscopy (SEM) has dramatically enhanced the understanding of cell wall structure and the different morphological forms of wood decay observed with light microscopy. The particles penetrated in the WAW can also be visible with SEM images. Furthermore, when combined with an energy-dispersive X-ray spectroscopy (EDS) system, SEM enables a comprehensive analysis of the inorganic chemical composition of the wood, thereby providing deeper insights into the degradation processes affecting wood[4,6,19–22].

Calcium and silicon are the most abundant elements found in WAW, primarily due to mineral compounds such as calcium carbonate/calcite ($CaCO_3$) and silicates/quartz (SiO_2) that seep into the wood from water. Additionally, iron and sulphur are commonly present in WAW. Sulphur naturally occurs in various environments and is derived from organic matter degradation or compounds released by human activities. The iron found in WAW typically originates from corroding nails, bolts, other construction materials, and weapons. Furthermore, ions of chlorine (Cl), copper (Cu), chromium (Cr), manganese (Mn), and zinc (Zn) are often detected in WAW, resulting from both natural environmental processes and human activities, including industrial development[23–28].

The changes that occur in WAW, along with the impacts of its underground environment, also affect materials other than wood used in shipbuilding, such as metal fasteners. Historical references well document metal nails made from copper, bronze, or iron. Numerous archaeological findings from various shipwrecks illustrate the application of these metal nails. The oldest archaeological evidence of metal nails in shipbuilding dates back to the wrecks discovered at Place Jules Verne (6th century BC) and Gela (500 BC)[29]. In addition to these, several shipwrecks constructed with iron nails have been discovered, such as the Kızılburun shipwreck (1st century BCE)[30], the Blackfriars ship (AD 130–175)[31], the Rugao ship (618–907), the Shiqiao ship (618-907), the Dazhi boat (960-1279), the Heyilu ship (960–1279), the Ningbo ship (960-1279), the Huaguang Reef No.1 shipwreck (960–1279), and the Penglai ships No.1, 2, and 3 (1271-1368), as well as the Xiangshan Ming Dynasty shipwreck (1368-1644) and the Shinan shipwreck (14th century)[32].

Some of the shipwrecks constructed with iron nails have undergone examinations to determine iron deposits within the wood, including the Lyon Saint Georges 4 shipwreck (2nd century)[33], the Quanzhou Ship (13th century)[34,35], the Mary Rose (16th century)[36], and the Vasa (17th century)[37] and Batavia (17th century)[38]. Furthermore, one of the iron nails from a shipwreck was analysed using X-ray diffraction (XRD). The examination of a corroded nail from the Dor 2006 Byzantine shipwreck (6-7th century) revealed the presence of magnetite (Fe_3O_4), indicating that the nail was initially made of iron[39].

The findings from this integrated approach significantly contribute to developing strategies for conserving WAW[21,40]. Between 2004 and 2013, salvage excavations conducted by the İstanbul Archaeological Museums in the Yenikapı quarter of İstanbul uncovered 37 shipwrecks dating from the 5th to the 11th centuries AD[41]. Among these, the Yenikapı (YK) 17 shipwreck studied in this paper is a compelling case study that illustrates the challenges and methodologies in conserving WAW. This paper investigates the physical and chemical properties of WAW samples collected from the YK 17 shipwreck and presents XRD analyses of the iron nails used in its construction.

Experimental

Materials and methods

YK 17 shipwreck represents one of the earliest and rare instances of a vessel not constructed with traditional planking methods within the Mediterranean region (Fig. 1). The hull structure was assembled using a hybrid construction method incorporating shell and skeleton techniques, illustrating the technological advancements in Mediterranean shipbuilding during the 1st millennium AD. A distinctive feature of YK 17 is its exclusive reliance on iron nails for assembly; all planks were secured to the frames using iron nails, and the futtocks and floor timbers were affixed to the substantial second wale with iron nails. YK 17 is notable for being the sole wreck excavated at Yenikapı with its ballast intact, which consisted of 56 stones (Fig. 2). The shipwreck measured 8.20 meters in length and 2.25 meters in width. It is dated to AD 652–870 through radiocarbon analyses[42,43]. Its primary components were constructed using species such as *Pinus L.* (pine) for thirty-nine wooden elements of the shipwreck and *Quercus L.* (oak) for five wooden elements[44].

Sampling

Nineteen WAW samples were selected as research subjects in the desalination tanks at the IU Yenikapı Shipwrecks Research Laboratory (Fig. 3). The WAW samples were chosen based on sampling availability, suitable size, and wood species. The primary techniques employed to assess the physical degradation of WAW are MWC, BD, and RBD. After calculating these values, the WAW samples were examined using FTIR, SEM, and SEM-EDS analyses. In addition to the WAW analyses, four iron nail samples were analysed using XRD (Fig. 4).

Sample preparation for loss of wood substance

MWC, BD, and RBD were identified as vital physical properties indicative of the degradation level of WAW. Samples weighing no less than 1 g were collected from locations not close to the iron corrosion products to determine the values.



Fig. 1 | Photo of the YK 17 shipwreck (© IU Yenikapı Shipwrecks Project Archive).



Fig. 2 | Photo of YK 17 shipwrecks *in situ* (© IU Yenikapı Shipwrecks Project Archive).

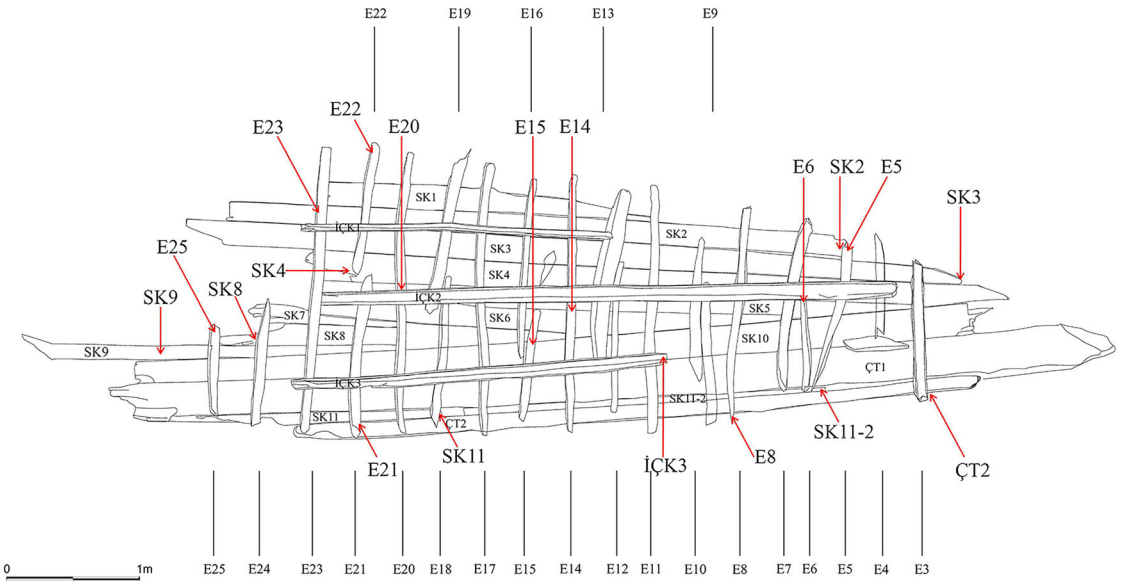

Fig. 3 | Schematic representation of the YK 17 shipwreck showing the sampling points (© IU Yenikapı Shipwrecks Project Archive).

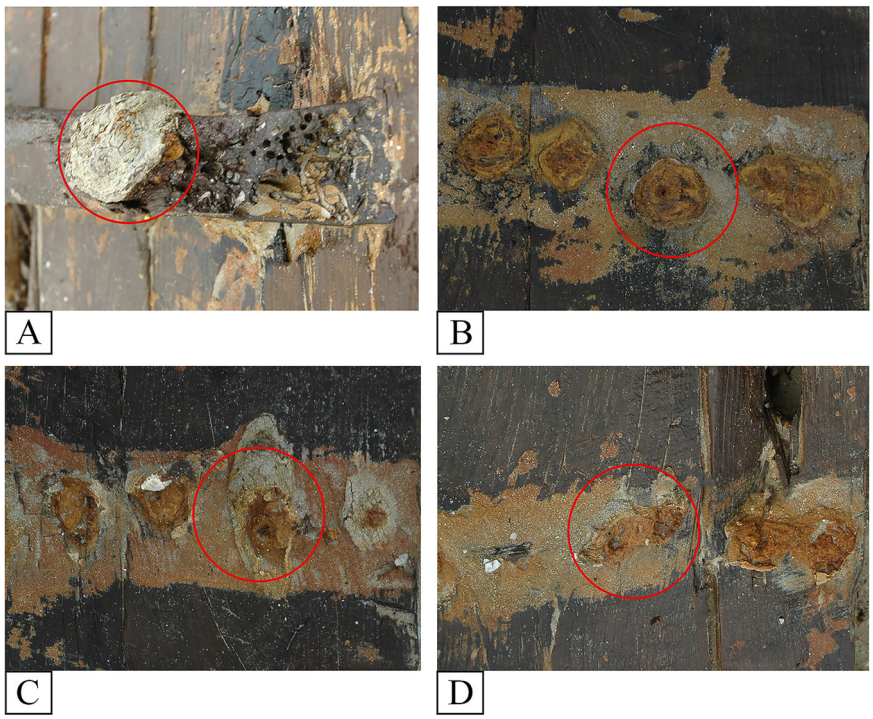

Fig. 4 | Photographs taken to illustrate the areas where iron nails were taken from the woods of the shipwrecks: (**A**) E25, (**B**) SK1, (**C**) SK1-2, and (**D**) SK9 (© IU Yenikapı Shipwrecks Project Archive).

Sample preparation for ATR-FTIR analyses

The wood samples were prepared into thin sections measuring approximately 4 mm in diameter for ATR-FTIR analyses. Furthermore, fresh pine and oak wood samples were collected for ATR-FTIR analyses to facilitate a comparison of the spectra between the WAW and the fresh wood samples.

Sample preparation for SEM and SEM-EDS

WAW samples were prepared in cross-sectional form (approximately 0.5–1 cm^3) using a razor blade for analysis via SEM and SEM-EDS.

Sample preparation for XRD

Iron nails from YK 17 shipwreck were powdered with an agate mortar to be analysed using XRD.

Methods

Loss of wood substance calculations

Before the measurement, the dirt on the surface of the samples was cleaned. Next, the WAW samples were weighed using a precision scale, and the weights of the WAW samples (Ww) were recorded. Then, the volume of the WAW samples (Vw) was measured (cm^3). Subsequently, the samples were oven-dried at 102 ± 3 °C, and the weight was recorded after three consecutive constant measurements as the weight of the oven-dry sample (Wd)[45–47]. Equation 1 was used to calculate MWC values, and Eq. 2 was used for BD. In order to assess the extent of wood degradation, the residual basic density (RBD) was determined as a percentage, calculated by comparing the measured density of the WAW to the average basic density of fresh wood of the same species, as reported in the literature. RBD values of the samples were obtained using Eq. 3.

$$MWC(\%) = \frac{\mathrm{Ww} - \mathrm{Wd}}{\mathrm{Wd}} \times 100 \quad (1)$$

$$BD = \frac{Wd}{Vw} \quad (2)$$

$$RBD(\%) = \frac{BD}{BD(fresh\ wood)} \times 100 \quad (3)$$

The classification of MWC values has been conducted by de De Jong[48]. The numerical categories align with the water content ranges of the samples as follows: (1) MWC > 400%, (2) MWC 185–400%, and (3) MWC < 185%.

ATR-FTIR

FTIR spectroscopy was performed utilizing a Perkin Elmer Spectrum UATR Two FTIR spectrometer equipped with an attenuated total reflection (ATR) sampling accessory. The spectra were the average of 16 scans recorded at a resolution of 4 cm^{-1} in the range from 4000 to 600 cm^{-1}. The FTIR spectra, presented as absorbance versus wavenumber, underwent baseline correction using the spectrum software.

SEM and SEM-EDS

In order to examine the physical degradation of the samples in detail, the samples were analysed using a QUANTA FEG 650 scanning electron microscope. SEM micrographs were taken under low vacuum without coating. In addition, energy-dispersive X-ray spectroscopy (EDS) was performed using an SDD Apollo X detector at a voltage of 20 kV on selected points of each sample. This method allows us to determine the elemental composition at the points of interest in the samples observed with SEM.

XRD

A Malvern PANalytical Empyrean MultiCore diffractometer (40 kV, 15 mA, CuKα1, 1.54059 Å) with a PIXcel3D detector was used over a two-theta range of 0° to 90° and with a run time of approximately 6 h. Data analysis was performed using Highscore software equipped with the JCPDS (Joint Committee on Powder Diffraction Standards) database for search-match functionality.

Results and discussion

The non-destructive analysis methods do not consistently yield reliable results, as they can be affected by air inclusions in intact fibres with non-degraded pits and cell walls[49]. Therefore, MWC, BD, and RBD values are presented (Table 1). When the values were examined, it could be seen that all the samples could be classified as Class I according to De Jong' Classification. The sample with the highest MWC value was oak, and the pine WAW samples had values lower than those of the oak WAW samples. In Fig. 5, the MWC values of the WAW samples showed a relationship with the condition of the wood, which was calculated as RBD (%). When Fig. 5 was examined, the effect of wood species on degradation became clearer. Although the MWC and BD values of samples E15 and E21 were the same, the RBD values differed because one sample was oak and the other was pine. Especially, MWC value calculation is a standard method to classify the woods from Yenikapı shipwrecks. Hundreds of woods were classified according to this method. It was determined that woods were highly degraded, degraded and well-preserved. Besides this, oak woods were generally better preserved than pine wood. In contrast, oak woods from Yenikapı 17 were highly degraded and classified as Class I, like pine woods[47,50–55].

Fourteen pine WAW samples, five oak WAW samples, and fresh wood samples of pine and oak were analysed using the ATR-FTIR method. To determine the chemical degradation of the WAW samples, the spectra of the WAW samples were compared with those of the fresh wood samples. The data evaluation was limited to the fingerprint region of the wood (1800–800 cm^{-1})[56].

The FTIR spectra of fresh pine and oak wood samples and the WAW samples were analysed (Figs. 6 and 7). Key observations include the peak at ~898 cm^{-1}[57], ~1105 cm^{-1}[58], ~ 1030 cm^{-1}[59], ~1044 cm^{-1}[60], ~1155 cm^{-1}[59] and ~1164 cm^{-1}[61], which are indicative of cellulose and hemicellulose. The ~898 and 1105 cm^{-1} bands were only detected in the spectra of the fresh pine and oak wood samples, not in the WAW samples. The peak at ~1030 cm^{-1}

Table 1 | The genus, MWC, BD and RBD values and condition of the WAW samples

Sample	Genus	MWC (%)	BD (g/cm^3)	RBD (%)	Condition (de Jong)
ÇT2	Pine	525	0.17	40	1
E5	Pine	609	0.15	36	1
E6	Pine	606	0.14	33	1
E8	Pine	721	0.13	31	1
E14	Oak	800	0.11	20	1
E15	Oak	585	0.14	25	1
E20	Oak	1150	0.08	14	1
E21	Pine	585	0.14	33	1
E22	Pine	403	0.21	50	1
E23	Oak	633	0.14	25	1
E25	Oak	1160	0.08	14	1
İÇK3	Pine	483	0.18	43	1
SK2	Pine	795	0.12	29	1
SK3	Pine	522	0.16	38	1
SK4	Pine	627	0.14	33	1
SK8	Pine	657	0.14	33	1
SK9	Pine	560	0.16	38	1
SK11	Pine	788	0.13	31	1
SK11-2	Pine	472	0,16	38	1

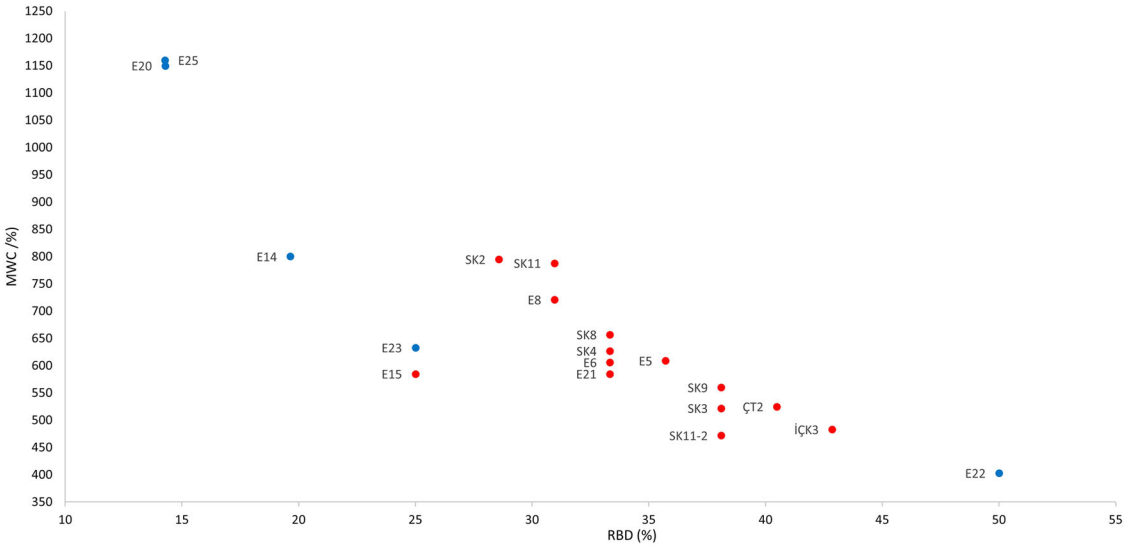

Fig. 5 | The MWC values of the samples in relation to the RBD values. (Blue dots represent oak WAW samples, and red dots represent pine WAW samples).

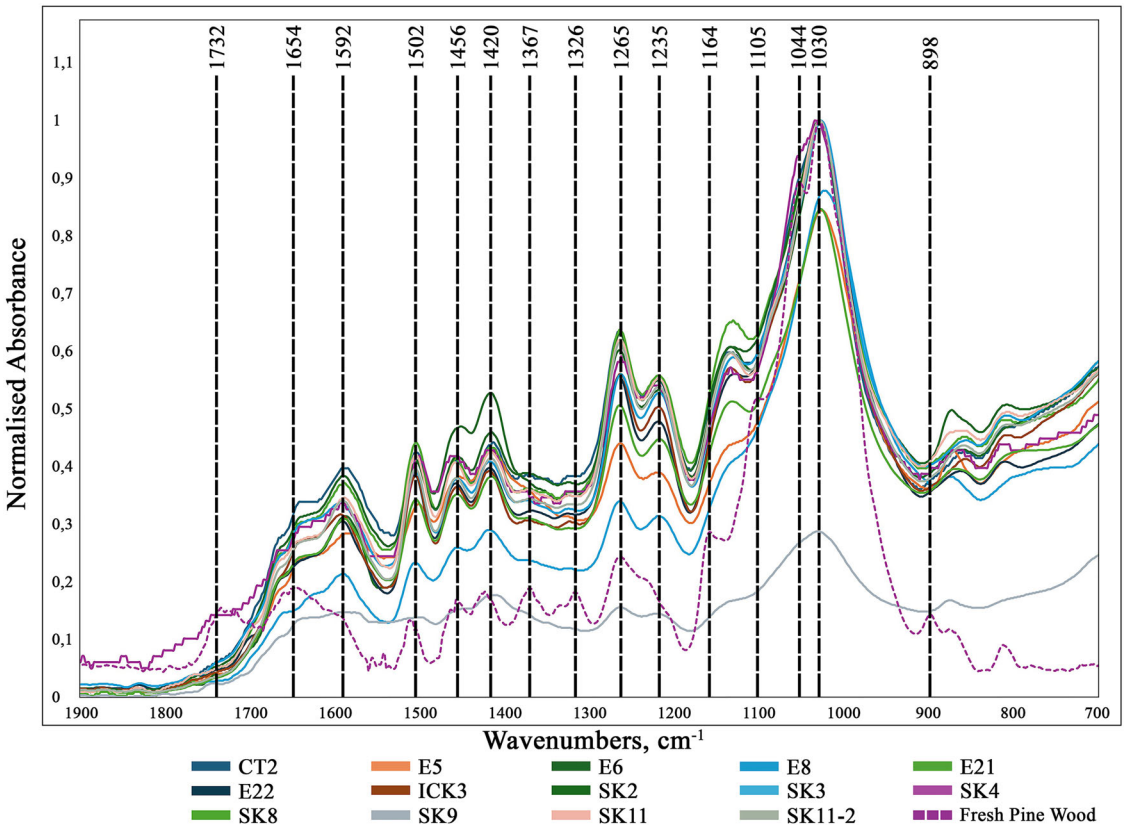

Fig. 6 | FTIR spectra of the pine WAW and fresh pine wood samples.

was detected in all spectra. Additionally, the bands at ~1044 and ~1164 cm^{-1} were only detected in the spectrum of fresh pine wood, not in the spectra of the pine WAW samples. There was a decrease in the intensity of the peak at ~1155 cm^{-1} in the spectra of the oak WAW samples, and this band was not detected in the spectra of the oak samples. The bands at ~1235 cm^{-1}[62], 1265 cm^{-1}[63], 1456 cm^{-1}[64], 1460 cm^{-1}[65], 1502 cm^{-1}[66], 1592 cm^{-1}[67] and 1654 cm^{-1}[65] are related to lignin. The band at ~1235 cm^{-1} was detected in all spectra except for the fresh oak wood spectrum. The peaks at ~1502, 1592 and 1654 cm^{-1} were detected in all spectra. The band at ~1216 cm^{-1} indicates an esterification of the wood[68] and was detected in the spectra of the oak WAW samples. The band at ~1265 cm^{-1} was detected in the spectra of the fresh pine and oak wood and the WAW pine wood samples, while the band at ~1460 cm^{-1} was found in the spectra of both fresh and WAW pine wood. The band at ~1456 cm^{-1} was detected in the fresh and WAW pine sample spectra. The band at ~1326 cm^{-1} is related to C-O vibration in syringyl rings and C-H bonds in cellulose[69]. The bands at ~1367 and 1420 cm^{-1} are related to cellulose[70]. The bands at ~1326 and 1420 cm^{-1} were detected in all spectra. When examining the band at ~1367 cm^{-1}, a decrease in the intensity of these

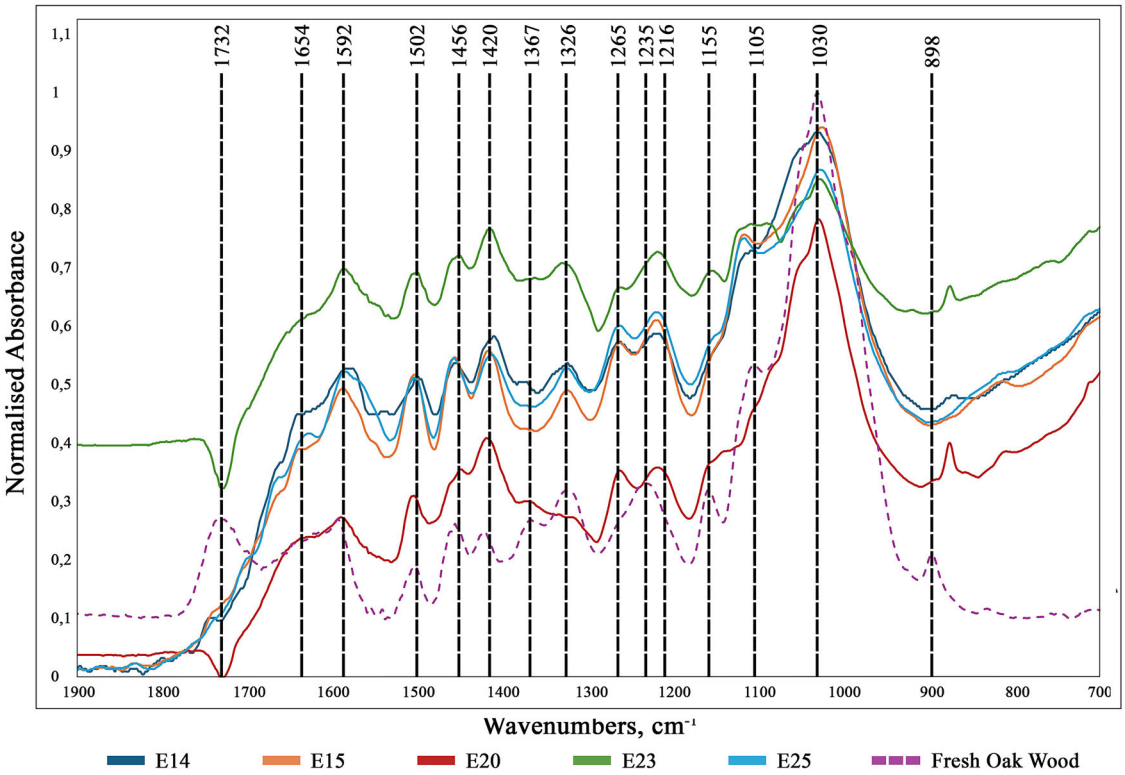

Fig. 7 | FTIR spectra of the oak WAW and fresh oak wood samples.

peaks in the WAW spectra was observed. Lastly, the band at ~1732 cm^{-1}[171] is associated with unconjugated carbonyl stretching in hemicellulose and was only detected in the fresh wood spectra, not in the WAW samples. Pine and oak samples from Yenikapı shipwrecks were investigated with FTIR and similar bands were detected, and their intensity, presence or absence have changed[18,54].

One of the methods used to assess the degradation occurring in the cells of WAW is scanning electron microscopy (SEM) imaging. Examination of Fig. 8A–C revealed that the tracheids suffered distortion and that the S2 layer of the fibers was nearly completely destroyed[72]. Significant physical changes, including collapse, disintegration, and ruptures, were observed in wood tracheid that had lost their original shapes (Fig. 8D–F). An intense collapse was noted in the tracheids of pine samples, where the tracheids from the spring and summer wood regions could be distinguished from one another (Fig. 8G–I). Additionally, physical degradation was found in the oak samples shown in Fig. 8J, where parenchyma cells were still clearly identifiable, as well as in Fig. 8K, L, where separations in cells and vessels were noted. SEM images examinations are consistent with the data obtained from MWC and FTIR analyses results. The data obtained from SEM images have revealed that the woods have undergone significant changes that are quite different from the original structure. It has been determined that the wood cavities (cell lumen) have lost their original shape. In addition, shrinkage and distortion have been detected in the samples. Moreover, Fig. 8K, L demonstrate the importance of using multiple techniques to investigate the WAW samples. Both images are from the same sample. Additionally, the more zoomed in images reveal a better preserved condition, despite the wood being highly degraded. Previous studies conducted on Yenikapı shipwrecks determined some very well preserved woods as well as degraded and highly degraded samples. In some woods from Yenikapı shipwrecks, major forms of microbial decay caused by erosion bacteria and soft rot fungi were determined[51,52,73,74].

While examining the SEM images of the WAW, observed particles were analysed using SEM-EDS (Fig. 9A–C). The particle detected in E6 mainly indicated S, Ca and Fe elements. In an image of the E15 sample, two particles were observed. The left indicated Si, S, Ca and Fe elements, and the right indicated Ca, Si, Al and Fe elements. The SEM image of the SK11-2 sample showed a tunnel created by *Teredo navalis*, which contained mainly Ca (Table 2). In former a study conducted on Yenikapı shipwrecks, particles have been found to primarily contain Fe due to iron corrosion products in the woods. In addition, S, Ca, and Si were also found[47,52,74].

Samples were investigated to determine the elemental structure of the woods, particularly the contamination of inorganic compounds inside the WAW samples (Table 2). An examination of the SEM-EDS data of the samples shown in Fig. 10A–C revealed that the samples primarily contained Ca, Fe, and S. Furthermore, the E22 and SK9 samples contained more Al than the E8 samples. A study conducted on Yenikapı shipwrecks found primarily Fe, S and Ca when the woods were analysed with SEM-EDS[51]. The detected elements, sulphur and calcium, mainly came from the marine environment, while the iron came from the iron nails components[75]. In addition, it is not uncommon to find calcium in wood fiber[76,77]. The presence of iron and other inorganic compounds in the WAW can causes problems while conservation process. Iron compounds in the WAW can be formed in iron(III)hydroxides and oxides, and reduced sulphur compounds. The WAW can face threats linked to inorganic compounds. These include potential mechanical damage from high levels of inorganic accumulation, the generation of acids from the oxidation of iron in reduced sulphur compounds that can degrade wood, and the catalytic effect of iron compounds that can initiate oxidative degradation, leading to the breakdown of wood components and preservation agents. Therefore, conservators have compelling reasons to remove or inactivate iron compounds in wood prior to conservation. Ethylenediamine tetraacetic acid (EDTA) can complex both iron and calcium, with its effectiveness depending on the solution's pH. One hypothesis suggests that iron and calcium may compete for complexation, or that all available iron is chelated first, followed by the formation of calcium-EDTA complexes. Further research is needed to fully understand the extraction of calcium and to evaluate the long-term effects of calcium removal on the integrity of the wood[77,78].

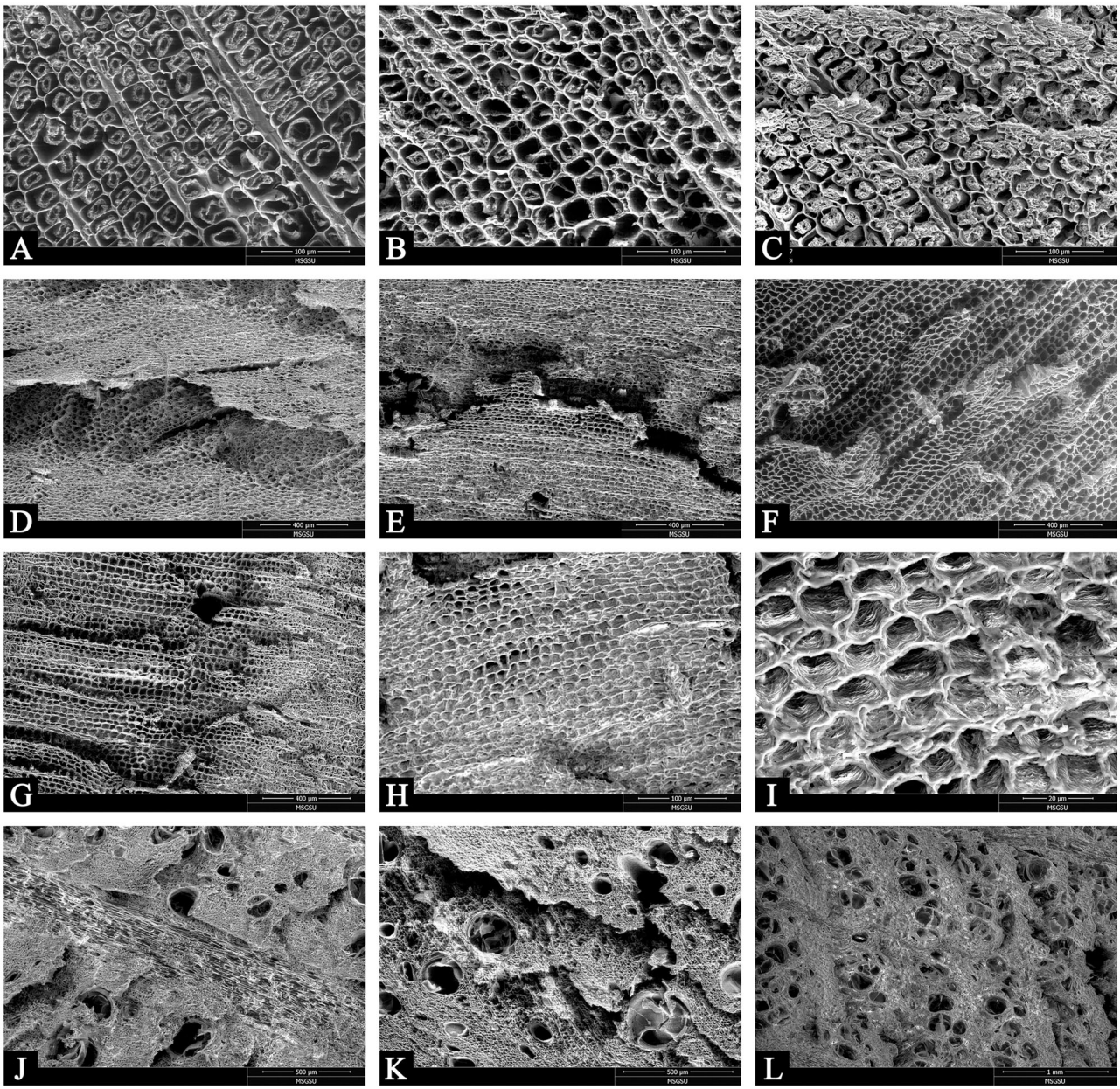

Fig. 8 | SEM images of the samples: E6, (**B**) ICK3, (**C**) SK11, (**D**) SK8, (**E**) SK9, (**F**) SK2, (**G**) E14, (**H**) E15, (**I**) E20, (**J**) E8, (**K**) and (**L**) E22.

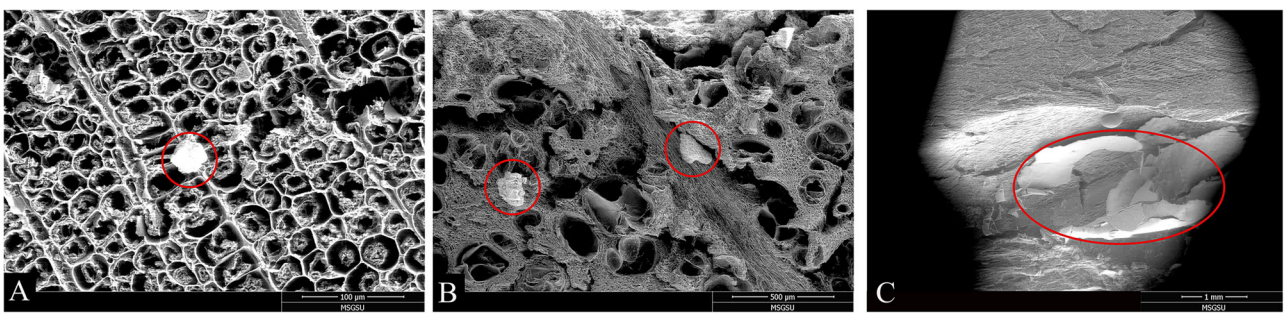

Fig. 9 | SEM-EDS data of the particles from the samples: (**A**) E6, (**B**) E15, and (**C**) SK11-2.

Four iron nails from the shipwreck woods (E25, SK1, SK1-2 and SK9) were analysed using XRD (Fig. 11). Goethite, iron oxide mineral (α-FeO(OH)) and calcite, calcium carbonate ($CaCO_3$)[79], were found in all samples. Goethite is the most common ingredient of iron rust and is normally formed under oxidizing conditions as a weathering product of iron minerals[80]. Precipitates of iron and sulphate salts, formed as oxidation products of iron(II) sulphides, are frequently found on surfaces of the drying wood, *e.g.* jarosite ($KFe_3(SO_4)_2(OH)_6$), melanterite ($FeSO_4{\cdot}7H_2O$), rozenite

Table 2 | SEM-EDS results of the analysed WAW samples and the particles detected in the samples

Sample	Al (%)	Ca (%)	Cl (%)	Fe (%)	K (%)	Mg (%)	Na (%)	P (%)	S (%)	Si (%)
Particle in E6	2.64	30.63	3.94	10.15	-	2.75	0.96	1.90	46.15	0.86
Particle in E15 (Left)	3.39	12.79	-	5.59	2.04	0.39	-	2.33	12.88	60.60
Particle in E15 (Right)	5.95	67.20	-	4.96	1.45	2.03	-	1.97	4.05	12.38
Particle in SK11-2	-	97.53	-	-	-	-	-	2.47	-	-
E6	1.67	27.66	4.99	13.47	2.85	2.60	1.39	2.71	40.44	2.22
E8	1.30	38.45	2.99	16.98	2.79	2.24	-	-	35.24	-
E15	2.73	36.77	4.95	11.73	2.03	3.76	-	2.99	31.69	3.36
E21	3.72	34.07	3.45	4.09	1.56	2.35	0.00	1.18	47.23	2.35
E22	7.46	36.43	6.76	5.99	5.23	1.44	-	-	36.68	-
İÇK3	0.00	33.36	5.71	2.71	2.76	3.76	2.10	1.76	46.54	1.31
SK2	2.46	40.05	4.40	11.63	2.85	2.01	-	-	36.60	-
SK3	2.67	38.62	8.99	4.61	4.77	0.75	-	-	39.59	-
SK8	-	26.87	-	20.86	-	2.43	1.55	2.33	43.56	2.40
SK9	8.08	22.20	4.28	18.57	1.63	1.73	-	2.68	37.97	2.86
SK11	11.01	31.25	4.81	8.64	3.54	2.40	-	-	38.36	-
SK11-2	-	30.98	-	2.44	-	3.91	1.64	1.96	57.96	1.11

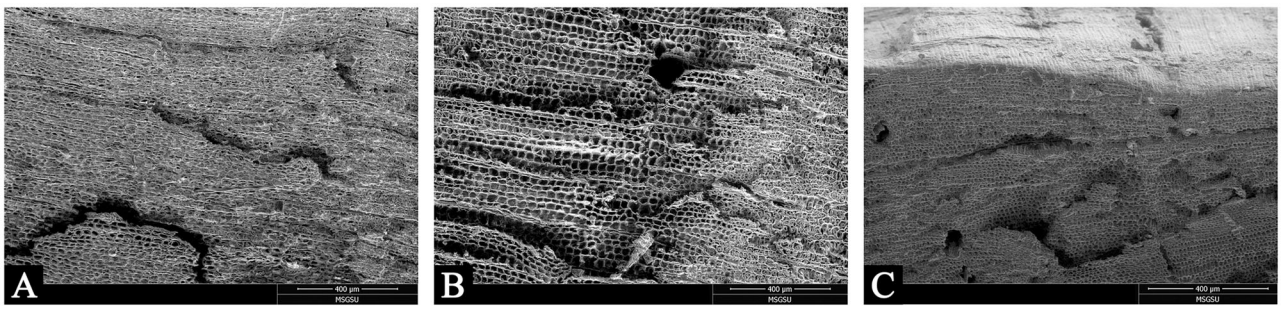

Fig. 10 | SEM-EDS data of the samples: (**A**) SK9, (**B**) E8, and (**C**) E22.

($FeSO_4{\cdot}4H_2O$) and gypsum ($CaSO_4{\cdot}2H_2O$), but also goethite, elemental sulphur (α-S8), magnetite (Fe_3O_4) and calcite[56,81–83]. In the corrosion products of the archaeological objects, the dominant phase in the corrosion products was goethite, whose presence can be related to the preservation of the base metal (iron). Calcite can form as a concretion outside the nail and/or as an integral part of the surrounding rocks, which may occur during the nail construction process[84]. Before this study, none of the metal nails from the Yenikapı shipwrecks were examined using XRD. On the other hand, dust particulates found in the woods of the Yenikapı 12 shipwreck were analysed with XRD in a previous study, and melanterite, rozenite and quartz were identified[85].

Conclusion

This study provided comprehensive insights into the degradation characteristics and chemical composition of pine and oak WAW samples from the YK 17 shipwreck through basic techniques, including maximum water content (MWC), basic density (BD), and relative basic density (RBD), as well as minimally invasive methods such as FTIR analysis, SEM, and SEM-EDS. The results revealed that the wood samples were classified as Class I according to De Jong's Classification. The MWC values of the oak WAW samples varied from 585 to 1160, while the values for the pine WAW samples ranged from 403 to 795. It was shown that oak wood samples generally possessed higher MWC values compared to pine samples. One of the interesting results of the study was the detection of an oak and a pine sample with the same MWC values; however, the difference in RBD values between these two samples serves as a clear example of how wood species affects degradation. The comparison of FTIR spectra highlighted the chemical degradation of WAW samples, showing a notable absence of key cellulose and hemicellulose peaks while indicating the chemical breakdown of the wood structure, whereas lignin components displayed greater durability.

Moreover, the SEM imaging elucidated the physical changes in the wood cells, highlighting the clear destruction of the S2 layer of fibres and the notable disintegration of tracheid. The SEM image examinations were consistent with the data obtained from the MWC results. Furthermore, the SEM images of the E22 WAW sample illustrate the importance of employing various techniques to examine WAW samples. Both images pertain to the same sample, and the higher magnification images reveal a better-preserved condition, despite the wood being severely degraded.

The elemental analysis via SEM-EDS provided crucial information about the contamination of inorganic compounds, revealing the presence of calcium and sulphur, likely sourced from the marine environment, as well as iron associated with the iron nails.

In addition to the analyses of WAW, the iron nails from the YK 17 shipwreck were examined using XRD. Prior to this study, the shipwreck had been classified as a vessel constructed from iron nails based on visual inspection. This study marks the first analysis of the chemical composition of the nails, determining the presence of goethite and calcite in the highly corroded nail samples via XRD analysis.

In conclusion, this research emphasized the complex interplay between biological and chemical degradation, as well as environmental influences, such as construction materials, on the degradation state of wood from the

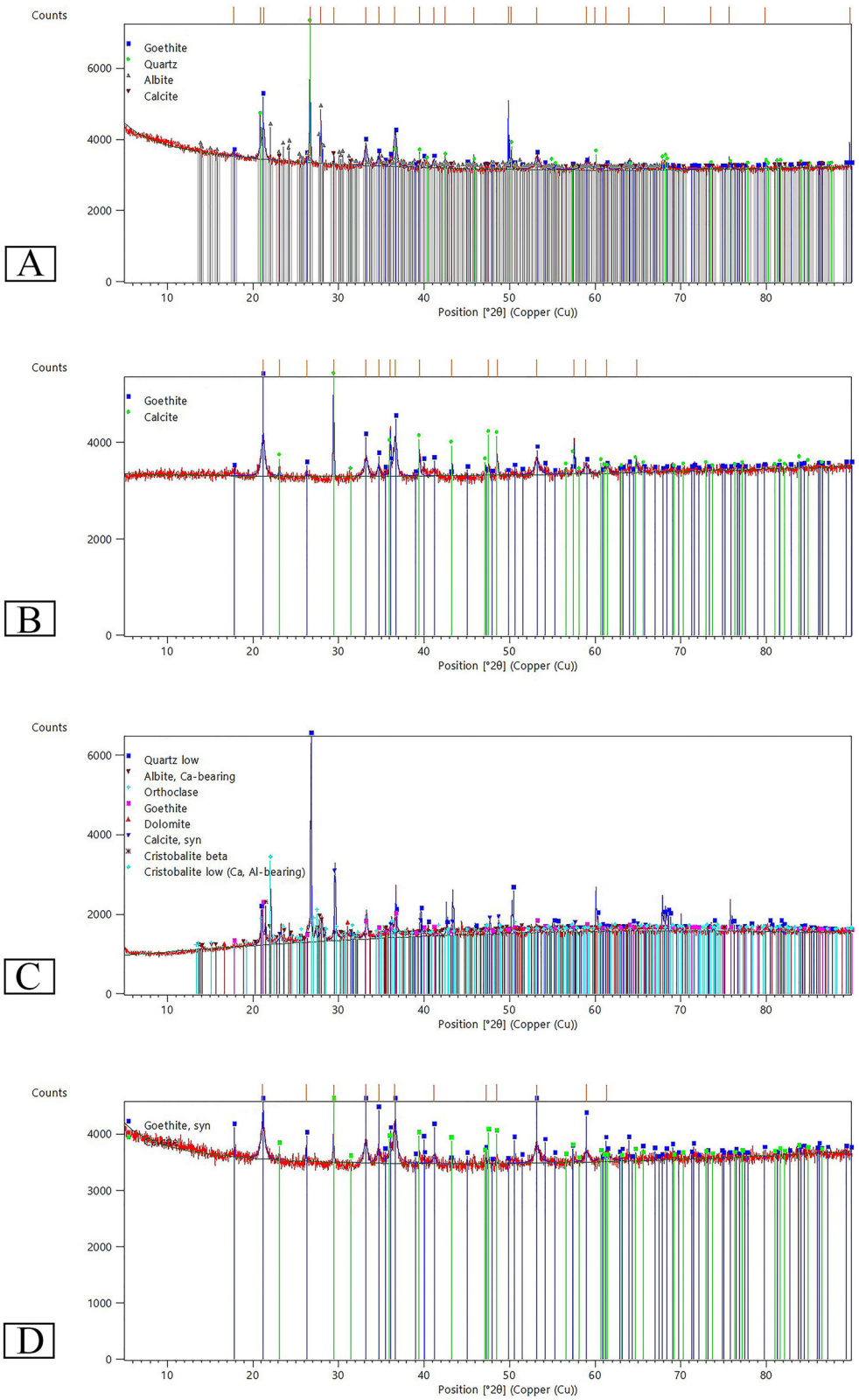

Fig. 11 | Search-match results for the XRD data collected from the nail samples: (**A**) E25, (**B**) SK1, (**C**) SK1-2, and (**D**) SK9.

YK 17 shipwrecks. Detailed studies on each of the 37 shipwrecks unearthed in Yenikapı will contribute to the internal evaluation of this group of shipwrecks. The results obtained herein can serve as valuable data for the assessment and conservation strategies of WAW, aiding the conservation efforts for these invaluable cultural heritage materials.

One of the primary methods used in the conservation of WAW is the polyethylene glycol (PEG) method, which is also the main method employed in the conservation of the Yenikapı shipwrecks. The molecular weight of the PEG is chosen based on the degradation level of the wood. Highly degraded wood is conserved using high molecular weight

PEG (PEG 2000, 3000, 3400, and 4000), whereas well-preserved wood is conserved with low molecular weight PEG (PEG 400). Based on the information collected about the shipwreck, it was determined that the conservation of the highly degraded wood should be conducted using high molecular weight PEG. The concentration of the PEG solution will be 10% at the beginning of the impregnation process. Then, the concentration of the PEG solution will be gradually increased by 10% to reach a final concentration of 45%. After PEG impregnation, the wood will be dried using a vacuum freeze dryer. In addition, the highly corroded iron nails found on the shipwreck should be cleaned using both mechanical and chemical methods prior to the impregnation process. Furthermore, due to the presence of iron that has penetrated into the wood, the iron compounds should be removed mechanically, and the wood will be treated with a disodium EDTA solution before being neutralised in distilled water.

Data availability

No datasets were generated or analysed during the current study.

Received: 27 September 2024; Accepted: 5 December 2024;
Published online: 06 March 2025

References

1. Florian M. L. E. Scope and history of archaeological wood. In: Rowell R. M., Barbour R. J., editors. Archaeol. wood Prop Chem Preserv. Washington, D.C: American Chemical Society. : 3–32. 1990 https://doi.org/10.1021/ba-1990-0225.ch001.
2. Jordan, B. A. Site characteristics impacting the survival of historic waterlogged wood: A review. *Int Biodeterior. Biodegrad* **47**, 47–54, https://doi.org/10.1016/S0964-8305(01)00035-X (2001).
3. Björdal, C. G. Microbial degradation of waterlogged archaeological wood. *J. Cult. Herit.* **13**, S118–S122, https://doi.org/10.1016/j.culher.2012.02.003 (2012).
4. Balzano, A., Merela, M. & Čufar, K. Scanning electron microscopy protocol for studying anatomy of highly degraded waterlogged archaeological wood. *Forests* **13**, 161, https://doi.org/10.3390/f13020161 (2022).
5. Hedges J. I. The chemistry of archaeological wood. In: Rowell R. M., Barbour R. J., editors. Archaeol. wood Prop Chem Preserv. Washington, D.C: American Chemical Society. 111-140. 1990 https://doi.org/10.1021/ba-1990-0225.ch005.
6. Broda, M. & Hill, C. A. S. Conservation of waterlogged wood—past, present and future perspectives. *Forests* **12**, 1193, https://doi.org/10.3390/f12091193 (2021).
7. Jensen, P. & Gregory, D. J. Selected physical parameters to characterize the state of preservation of waterlogged archaeological wood: A practical guide for their determination. *J. Archaeol. Sci.* **33**, 551–559, https://doi.org/10.1016/j.jas.2005.09.007 (2006).
8. Pizzo, B., Giachi, G. & Fiorentino, L. Reasoned use of chemical parameters for the diagnostic evaluation of the state of preservation of waterlogged archaeological wood. *J. Archaeol. Sci.* **40**, 1673–1680, https://doi.org/10.1016/j.jas.2012.12.003 (2013).
9. Grattan D. W. Waterlogged Wood. In Conservation of Marine Archaeological Objects; Pearson C. (editor). Butterworth & Co. (Publishers) Ltd: London, UK, 55–67 1987.
10. Schniewind A. P. Physical and mechanical properties of archaeological wood. In: Rowell R. M., Barbour R. J., editors. Archaeol. wood Prop Chem Preserv. Washington, D.C: American Chemical Society. 87–109. https://doi.org/10.1021/ba-1990-0225.ch004 (1990).
11. Babiński, L., Fabisiak, E., Zborowska, M., Michalska, D. & Prądzyński, W. Changes in oak wood buried in waterlogged peat: shrinkage as a complementary indicator of the wood degradation rate. *Eur. J. Wood Wood Products* **77**, 691–703, https://doi.org/10.1007/s00107-019-01420-z (2019).
12. Macchioni, N., Pecoraro, E. & Pizzo, B. The measurement of maximum water content (MWC) on waterlogged archaeological wood: A comparison between three different methodologies. *J. Cult. Herit.* **30**, 51–56, https://doi.org/10.1016/j.culher.2017.10.005 (2018).
13. Singh, A. P., Kim, Y. S. & Chavan, R. R. Advances in understanding microbial deterioration of buried and waterlogged archaeological woods: A review. *Forests* **13**, 394, https://doi.org/10.3390/f13030394 (2022).
14. Giachi, G., Bettazzi, F., Chimichi, S. & Staccioli, G. Chemical characterisation of degraded wood in ships discovered in a recent excavation of the Etruscan and Roman Harbour of Pisa. *J. Cult. Herit.* **4**, 75–83, https://doi.org/10.1016/S1296-2074(03)00018-9 (2003).
15. Pizzo B., Macchioni N., Alves A. Characterization of waterlogged wood by infrared spectroscopy. In Wood science for conservation of cultural heritage-Braga 2008: proceedings of the international conference held by Cost action IE0601 in Braga (Portugal) 5-7 November 2008. Firenze University Press. 1000-1006 (2010).
16. Chan, K. A. & Kazarian, S. G. Attenuated total reflection Fourier-transform infrared (ATR-FTIR) imaging of tissues and live cells. *Chem. Soc. Rev.* **45**, 1850–1864 (2016).
17. Akyüz, S. Investigation of the degradation stages of archaeological and historic silk textiles: An ATR-FTIR spectroscopic study. *Archaeol. Anthropol.* **3-1**, 447–451 (2018).
18. Kılıç, A. G. & Kılıç, N. Application of FTIR spectroscopy to the characterization of waterlogged archaeological woods of three galleys from Yenikapi, Istanbul: Contribution to conservation. *Mediterr. Archaeol. Archaeom.* **21**, 93–105, https://doi.org/10.5281/zenodo.4681734 (2021).
19. Blanchette R., Nilsson T., Daniel G., Abad A. R. Biological degradation of wood. In: Rowell R. M., Barbour R. J., editors. Archaeol wood Prop Chem Preserv. Washington, D.C: American Chemical Society: 141–174 https://doi.org/10.1021/ba-1990-0225.ch006 (1990).
20. Powell, K. L., Pedley, S., Daniel, G. & Corfield, M. Ultrastructural observations of microbial succession and decay of wood buried at a Bronze Age archaeological site. *Int Biodeterior. Biodegrad* **47**, 165–173, https://doi.org/10.1016/S0964-8305(01)00045-2 (2001).
21. Giachi, G., Capretti, C., Macchioni, N., Pizzo, B. & Donato, I. D. A methodological approach in the evaluation of the efficacy of treatments for the dimensional stabilisation of waterlogged archaeological wood. *J. Cult. Herit.* **11**, 91–101, https://doi.org/10.1016/j.culher.2009.04.003 (2010).
22. Chadwick, A. V. et al. The application of X-ray absorption spectroscopy in archaeological conservation: Example of an artefact from Henry VIII warship, the Mary Rose. *J. Non-Cryst. Solids* **451**, 49–55, https://doi.org/10.1016/j.jnoncrysol.2016.05.020 (2016).
23. Fors, Y. & Sandström, M. Sulfur and iron in shipwrecks cause conservation concerns. *Chem. Soc. Rev.* **35**, 399–415 (2006).
24. Rémazeilles, C., Tran, K., Guilminot, E., Conforto, E. & Refait, P. Study of Fe(II) sulphides in waterlogged archaeological wood. *Stud. Conserv* **58**, 297–307, https://doi.org/10.1179/2047058412Y.0000000071 (2013).
25. Fors, Y. et al. Sulfur and iron accumulation in three marine-archaeological shipwrecks in the Baltic Sea: the ghost, the crown and the sword. *Sci. Rep.* **4**, 4222 (2014).
26. Broda, M. & Frankowski, M. Determination of the content of selected elements in medieval waterlogged oak wood from the Lednica Lake—a case study. *Environ. Sci. Pollut. R.* **24**, 23401–23410 (2017).
27. Schweingruber F. H., Börner A. Fossilization, permineralization, coalification, carbonization and wet wood conservation. In: Schweingruber F. H., Börner A. (eds) The plant stem: a microscopic aspect. Springer International Publishing, Cham. 183–192. 2018
28. Broda, M., Jakes, J. E., Li, L. & Antipova, O. A. Archeological wood conservation with selected organosilicon compounds studied by XFM and nanoindentation. *Wood Sci. Technol.* **57**, 1277–1298, https://doi.org/10.1007/s00226-023-01503-4 (2023).

29. Kahanov, Y., Doherty, C. & Shalev, S. The metal nails from the Ma'agan Mikhael ship. *Int J. Nautical Archael* **28**, 277–288, https://doi.org/10.1016/S1057-2414(99)80051-X (1999).
30. Littlefield J. D. The hull remains of the late Hellenistic Shipwreck at Kızılburun, Turkey. Texas A&M University. Master's Thesis. 2012.
31. https://www.heritagegateway.org.uk/Gateway/Results_Single.aspx?uid=405065&resourceID=19191, Accessed 28 August 2024.
32. Kimura J. Historical development of shipbuilding technologies in East Asia. Shipwreck ASIA: Thematic Stud in East Asian maritime archaeol. Adelaide: Maritime Archaeol Prog, 1-25. 2015
33. Rémazeilles, C. et al. Post-treatment study of Iron/Sulfur-containing compounds in the wreck of Lyon Saint-Georges 4 (Second Century ACE). *Stud. Conserv* **65**, 28–36, https://doi.org/10.1080/00393630.2019.1610608 (2020).
34. Green, J. & Burningham, N. Museum of Overseas Communication History. The ship from Quanzhou, Fujian Province, People's Republic of China. *Inter J. Nautical Archaeol.* **27**, 277–301, https://doi.org/10.1016/S1057-2414(98)80001-0 (1998).
35. Green, J. N. The Song Dynasty shipwreck at Quanzhou, Fujian Province, People's Republic of China. *IJNA* **12**, 253–261, https://doi.org/10.1111/j.1095-9270.1983.tb00140.x (1983).
36. Smith A. D. et al. An investigation of the sulfur–iron chemistry in timbers of the sixteenth century warship, the Mary Rose, by synchrotron micro-X-Ray spectroscopy. In: Turbanti-Memmi, I. (eds) Proceedings of the 37th International Symp on Archaeom, 13th - 16th May 2008, Siena, Italy. Springer, Berlin, Heidelberg. 2011. https://doi.org/10.1007/978-3-642-14678-7_56.
37. Rose K. J. The naval architecture of Vasa, a 17th-century Swedish warship. Texas A&M University. PhD thesis. 2014.
38. Daly, A., Domínguez-Delmás, M. & van Duivenvoorde, W. Batavia shipwreck timbers reveal a key to Dutch success in 17th-century world trade. *Plos one* **16**, e0259391 (2021).
39. Kahanov, Y. et al. Archaeometallurgical analysis of metal remains from the Dor 2006 shipwreck: A clue to the understanding of the transition in ship construction. *J. Archaeol. Sci: Rep.* **2**, 321–332, https://doi.org/10.1016/j.jasrep.2015.02.013 (2015).
40. Giachi G., Macchioni N., Pizzo B., Capretti C. The waterlogged wood of the shipwrecks found in Pisa (Italy). Diagnosis and conservation, Proceedings of "Shipwrecks": 78-84. 2011
41. Kocabaş, U., Kılıç, N. & Asal, R. Keeping the past alive: The Yenikapi shipwrecks. *TINA* **14**, 14–55 (2020).
42. Türkmenoğlu, E. The Yenikapi 17 shipwreck found in the harbour of Theodosius and preliminary results on its construction technology. *ART-Sanat.* **9**, 23–33 (2018). (in Turkish).
43. Kocabaş, U. The Yenikapi Byzantine-Era Shipwrecks, Istanbul, Turkey: a preliminary report and inventory of the 27 wrecks studied by Istanbul University. *IJNA* **44**, 5–38 (2015).
44. Akkemik Ü. Woods of Yenikapı shipwrecks, Yenikapı shipwrecks. Istanbul, Turkey: Ege Publishing. II 2015.
45. Babinski, L., Izdebska, MunchaD. & Waliszewska, B. Evaluation of the state of preservation of waterlogged archaeological wood based on its physical properties: basic density vs. wood substance density. *J. Archaeol. Sci.* **46**, 372–383, https://doi.org/10.1016/j.jas.2014.03.038 (2014).
46. Kılıç, N. & Kılıç, A. G. Analysis of waterlogged woods. *Ex. Yenikapı shipwrecks. Art.-Sanat.* **9**, 1–11 (2014).
47. Kılıç, N. & Kılıç, A. G. Physical properties for the characterization of waterlogged archaeological wood of eight Yenikapı shipwrecks from Byzantine period. *Mediterr. Archaeol. Archaeom.* **19**, 133–148, https://doi.org/10.5281/zenodo.3364819 (2019).
48. De Jong, J. Conservation techniques for old waterlogged wood from shipwrecks found in the Netherlands. *Biodeterior. Invest Tech.* **113**, 295–338 (1977).
49. Stelzner, J. et al. Stabilisation of waterlogged archaeological wood: the application of structured-light 3D scanning and micro computed tomography for analysing dimensional changes. *Herit. Sci.* **10**, 60, https://doi.org/10.1186/s40494-022-00686-6 (2022).
50. Kılıç N. A research for the conservation treatment to be used on Yenikapi 12 shipwreck, and the conservation application for the shipwreck. Istanbul University. Master's thesis. 2013 (in Turkish).
51. Kılıç N. Assessment of pre-impregnation with polyethylene glycol and vacuum freeze drying method for the conservation of Yenikapı shipwrecks. Istanbul University. PhD thesis. 2017 (in Turkish).
52. Kılıç A. G. Sulphur and iron analysis together with their distribution in woods and their removal from the woods of Yenikapı shipwrecks. Istanbul University. PhD thesis. 2017 (in Turkish).
53. Akgün C. The investigation of degradation degree of Yenikapı 29 shipwreck and conservation proposal. İstanbul University. Master's thesis. 2020 (in Turkish).
54. Öztürk S. Evaluation of physical, chemical, and biological degradation of Yenikapı 16 shipwreck and the conservation proposal. Istanbul University. Master's thesis. 2021 (in Turkish).
55. Kılıç, A. G. Evaluation of the physical condition of a group of waterlogged woods from the shipwreck Yenikapi 35. *ART-SANAT* **9**, 13–21 (2018). (in Turkish).
56. Fors, Y., Jalilehvand, F. & Sandström, M. Analytical aspects of waterlogged wood in historical shipwrecks. *Anal. Sci.* **27**, 785–792, https://doi.org/10.2116/analsci.27.785 (2011).
57. Pandey, K. K. & Pitman, A. J. FTIR studies of the changes in wood chemistry following decay by brown-rot and white-rot fungi. *Inter Biodeterior. Biodegradat* **52**, 151–160, https://doi.org/10.1016/S0964-8305(03)00052-0 (2003).
58. McLean, J. P., Jin, G., Brennan, M., Nieuwoudt, M. K. & Harris, P. J. Using NIR and ATR-FTIR spectroscopy to rapidly detect compression wood in Pinus radiata. *Can. J. For. Res* **44**, 820–830, https://doi.org/10.1139/cjfr-2013-0329 (2014).
59. Naumann A., Peddireddi S., Kües U., Polle A. Fourier Transform Infrared Microscopy in Wood Analysis. In: Kües U. (editor) Wood production, wood technology, and biotechnological impacts, 179-196. 2007
60. Pucetaite M. Archaeological wood from the Swedish warship Vasa studied by infrared microscopy, Lund University. Master of Art Thesis. 2012.
61. Viet, D. Q. et al. Study on characteristics of acacia wood by FTIR and thermogrametric analysis. *Vietnam J. Chem.* **55**, 259–264, https://doi.org/10.15625/2525-2321.2017-00456 (2017).
62. Müller, G., Schöpper, C., Vos, H., Kharazipour, A. & Polle, A. FTIR-ATR spectroscopic analyses of changes in wood properties during particle-and fibreboard production of hard-and softwood trees. *BioResources* **4**, 49–71, https://doi.org/10.15376/biores.4.1.49-71 (2009).
63. Shi, J., Xing, D. & Lia, J. FTIR studies of the changes in wood chemistry from wood forming tissue under inclined treatment. *Energy Procedia* **16**, 758–762, https://doi.org/10.1016/j.egypro.2012.01.122 (2012).
64. Fackler, K. et al. Localisation and characterisation of incipient brown-rot decay within spruce wood cell walls using FT-IR imaging microscopy. *Enzym. Microb. Tech.* **47**, 257–267, https://doi.org/10.1016/j.enzmictec.2010.07.009 (2010).
65. Moosavinejad, S. M., Madhoushi, M., Vakili, M. & Rasouli, D. Evaluation of degradation in chemical compounds of wood in historical buildings using FT-IR and FT-Raman vibrational spectroscopy. *Maderas, Cienc. y. Tecnol.ía* **21**, 381–39, https://doi.org/10.4067/S0718-221X2019005000310 (2019).
66. Pandey, K. K. A study of chemical structure of soft and hardwood and wood polymers by FTIR spectroscopy. J Appl Polymer. *Sci* **71**, 1969–1975 (1999).
67. Zborowska, M., Stachowiak Wencek, A. & Waliszewska, B. Prądzyński W. Colourimetric and FT-IR ATR spectroscopy studies of degradative effects of ultraviolet light on the surface of exotic ipe (Tabebuia sp.) wood. *Cellul. Chem. Tech.* **50**, 71–76 (2016).

68. Giridhar, N., Pandey, K. K., Prasad, B. E., Bisht, S. S. & Vagdevi, H. M. Dimensional stabilization of wood by chemical modification using isopropenyl acetate. *Maderas, Cienc. y. Tecnol.ía* **19**, 15–20, https://doi.org/10.4067/S0718-221X2017005000002 (2017).
69. Traoré, M., Kaal, J. & Cortizas, A. M. Differentiation between pine woods according to species and growing location using FTIR-ATR. *Wood Sci. Tech.* **52**, 487–504, https://doi.org/10.1007/s00226-017-0967-9 (2018).
70. Hospodarova, V., Singovszka, E. & Stevulova, N. Characterization of cellulosic fibers by FTIR spectroscopy for their further implementation to building materials. *Am. J. Anal. Chem.* **9**, 303–310, https://doi.org/10.4236/ajac.2018.96023 (2018).
71. Kubovský, I., Kačíková, D. & Kačík, F. Structural changes of oak wood main components caused by thermal modification. *Polymers* **12**, 484–496, https://doi.org/10.3390/polym12020485 (2020).
72. Nguyen, T. D., Kohdzuma, Y., Endo, R. & Sugiyama, J. Evaluation of chemical treatments on dimensional stabilization of archeological waterlogged hardwoods obtained from the Thang Long Imperial Citadel site, Vietnam. *J. Wood Sci.* **64**, 436–443, https://doi.org/10.1007/s10086-018-1719-7 (2018).
73. Kılıç, A. G., Kılıç, N. & Akgün, C. The importance of using multiple analyses techniques to determine the physical condition of the waterlogged wood. *Wood Res.* **66**, 1046–1054, https://doi.org/10.37763/wr.1336-4561/66.6.10461054 (2021).
74. Köse C., Taylor A. M. Preliminary evaluation of degradation patterns in wood samples form the Yenikapı Shipwrecks. Inter Res Group on Wood Protection 44th Annual Meeting, Sweden: 1–11. 2013
75. Wang, X. & Li, N. Extraction of soluble salts and iron sulfides from the wood of the "Huaguangjiao I" Shipwreck. *Forests* **14**, 2432, https://doi.org/10.3390/f14122432 (2023).
76. Winandy J. E., Rowell R. M. Chemistry of wood strength. In: Rowell R. M. editor. Handbook of wood chemistry and wood composites. CRC Press, 303–347 https://doi.org/10.1021/ba-1984-0207.ch005 (2005).
77. Monachon, M. et al. Assessing the versatility of bioextraction to preserve waterlogged wood. *Forests* **14**, 1656, https://doi.org/10.3390/f14081656 (2023).
78. Almkvist G., Norbakhsh S., Persson I., Sahlstedt M., Hocker E. Extraction of iron compounds from archaeological wood – results and experiences from the Vasa Museum. Proceedings of the 12th ICOM-CC Wet Org Archaeol Mater Conference, Istanbul. 194–196 (2013).
79. Dietrich R. V. Calcite. In Encyclopedia Britannica, 5 Jun. 2024. https://www.britannica.com/science/calcite. Accessed 29 August 2024.
80. Britannica, The Editors of Encyclopaedia. Goethite. In Encyclopedia Britannica, 9 Jan. 2019. https://www.britannica.com/science/goethite. Accessed 29 August 2024.
81. Sandström, M. et al. Deterioration of the seventeenth-century warship Vasa by internal formation of sulphuric acid. *Nature* **415**, 893–897, https://doi.org/10.1038/415893a (2002).
82. Sandström, M. et al. Sulfur accumulation in the timbers of King Henry VIII's warship Mary Rose: A pathway in the sulfur cycle of conservation concern. *Proc. Natl. Acad. Sci. USA.* **102**, 14165–14170, https://doi.org/10.1073/pnas.0504490102 (2005).
83. Wetherall, K. M. et al. Sulfur and iron speciation in recently recovered timbers of the Mary Rose revealed via X-ray absorption spectroscopy. *J. Archaeol. Sci.* **35**, 1317–1328, https://doi.org/10.1016/j.jas.2007.09.007 (2008).
84. Jegdić, B., Polić, S., Ristic, S. & Alil, A. Corrosion Stability of Corrosion Products on an Archaeological Iron Artefact. *Inter J. Conserv Sci.* **3**, 241–248 (2012).
85. Kılıç, A. G., Kılıç, N. & Arnold, D. C. Analyses of sulfur and iron in waterlogged archaeological wood: The case of polyethylene-glycol-treated Yenikapı 12 shipwreck. *Forests* **14**, 1–12, https://doi.org/10.3390/f14030530 (2023).

Acknowledgements

The author acknowledges Prof. Dr. Ufuk Kocabaş, Prof. Dr. Ünal Akkemik, Prof. Dr. Namık Aysal, Assoc. Prof. Dr. A. Gökçe Kılıç, Istanbul Archaeology Museums, Yenikapı Shipwrecks Project Team, Scientific Research Projects Coordination Unit of Istanbul University (Project ID:39374), and TÜBA (Turkish Academy for Sciences) for their help and support. This study was funded by the Scientific Research Projects Coordination Unit of Istanbul University (Project ID:39374), with additional open access funding provided by TÜBA (Turkish Academy for Sciences).

Author contributions

The author wrote the manuscript.

Competing interests

The author declares no competing interests.

Additional information

Correspondence and requests for materials should be addressed to Namık KILIÇ.

Reprints and permissions information is available at http://www.nature.com/reprints

Publisher's note Springer Nature remains neutral with regard to jurisdictional claims in published maps and institutional affiliations.

Open Access This article is licensed under a Creative Commons Attribution-NonCommercial-NoDerivatives 4.0 International License, which permits any non-commercial use, sharing, distribution and reproduction in any medium or format, as long as you give appropriate credit to the original author(s) and the source, provide a link to the Creative Commons licence, and indicate if you modified the licensed material. You do not have permission under this licence to share adapted material derived from this article or parts of it. The images or other third party material in this article are included in the article's Creative Commons licence, unless indicated otherwise in a credit line to the material. If material is not included in the article's Creative Commons licence and your intended use is not permitted by statutory regulation or exceeds the permitted use, you will need to obtain permission directly from the copyright holder. To view a copy of this licence, visit http://creativecommons.org/licenses/by-nc-nd/4.0/.

© The Author(s) 2025